Direct measurement of the dispersion of the electrogyration coefficient of photorefractive $Bi_{12}GeO_{20}$ crystals

N. C. Deliolanis,[a] I. M. Kourmoulis, G. Asimellis, A. G. Apostolidis, and E. D. Vanidhis
Department of Physics, Aristotle University of Thessaloniki, Solid State Section 313-1, GR 54124 Thessaloniki, Greece

N. A. Vainos
National Hellenic Research Foundation (NHRF), Theoretical and Physical Chemistry Institute (TPCI), 48 Vassileos Constantinou Avenue, GR 11635 Athens, Greece

(Received 3 May 2004; accepted 11 October 2004; published online 27 December 2004)

We report on the direct measurement of the electrogyration coefficient of $Bi_{12}GeO_{20}$ sillenite crystals over the visible spectral range. The coefficient is directly measured on a (111)-cut crystal for which the electro-optic and electrogyratory effects are decoupled. The precision of the measurement method over various parameters including absorption and misorientation is examined. The value of the electrogyration coefficient is found to vary from 0.37 ± 0.03 to 0.05 ± 0.01 pm/V for the 460–760-nm spectrum range, which is within the upper boundaries that have been specified in previous experiments. It is also found that the electrogyration coefficient follows the dispersion law of optical activity and refractive index. © *2005 American Institute of Physics*.
[DOI: 10.1063/1.1828585]

I. INTRODUCTION

The photorefractive crystals of the sillenite class 23 [$Bi_{12}SiO_{20}$(BSO), $Bi_{12}GeO_{20}$(BGO), $Bi_{12}TiO_{20}$(BTO)] have been extensively studied and used in optical signal processing and interferometric applications (Refs. 1–3 and references therein). The sillenites exhibit natural optical activity (OA), the electro-optic (EO), and the electrogyratory (EG) effect.[4] In the EG effect, an applied electric field induces rotation of the polarization plane of a beam transmitted through a crystal. The effect is described by a third-rank axial tensor.[5] For crystal class 23 there is only one nonzero independent electrogyration coefficient ζ.

Over the last three decades various studies on the electrogyration of sillenites have been presented. Lenzo and co-workers[6–8] and Miller[9] have measured the rotation of the polarization plane under the influence of an electric field in $(\bar{1}10)$-cut BSO and BGO crystals. For this specific crystal configuration the polarization plane rotation was later attributed to the EO effect only.[10] In order to measure the electrogyration coefficient, the EO and the EG effect should be decoupled. Anastassakis[11] suggested that when light propagates in the [111] direction and an electric field is applied along the same direction, the polarization rotation induced by the EO effect is eliminated and, consequently, the EG effect can be observed and measured directly. This configuration has been used by Vlokh and Zarik[12] who successfully measured the electrogyration coefficient of BSO at 633 nm. They did not, however, detect the phenomenon in BGO. Tayag *et al.*[13] also were not able to observe the effect at all due to the coarse precision of their experiment. Further studies concerning the indirect measurement of the electrogyratory effect in (110)-cut sillenites by indirectly decoupling EO and EG effects have either reported a specific value[14–16] or an upper boundary.[17]

We directly measure the EG effect over the visible spectral range (460–760 nm). We present, first, a short theoretical analysis on the propagation of light along the [111] direction for a sillenite crystal under the influence of an electric field. Second, the experimental measurement of the EG coefficient and a discussion on the accuracy of the method follows. Finally, we present a comparison of our results with theoretical predictions and other experimental results found in the literature.

II. THEORETICAL ANALYSIS

The propagation of a light beam with wave normal **k** into an anisotropic material is examined with the help of the impermeability B_{ij} and the gyration g_{mn} tensors.[18–20] The electric field E_k perturbs the real part of the impermeability B_{ij}^o and the gyration g_{mn}^o tensor elements

$$B_{ij}^{\mathrm{re}} = B_{ij}^o + r_{ijk}E_k,$$

and

$$g_{mn} = g_{mn}^o + \zeta_{mnk}E_k, \tag{1}$$

where r_{ijk} and ζ_{mnk} are the electro-optic and the electrogyration tensor elements, respectively. Here, r is the effective EO coefficient, including both the primary and the secondary (piezoelectric and photoelastic) effects.[18] In group 23, both tensors have the same symmetry and their nonzero elements in contracted notation are[4,18,19] $r_{41}=r_{52}=r_{63}=r$ and $\zeta_{41}=\zeta_{52}=\zeta_{63}=\zeta$. In the case of no absorption, the complex impermeability tensor B is Hermitian,

[a]Electronic mail: optlab@auth.gr

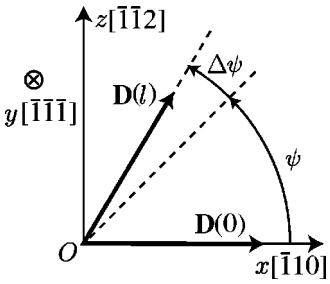

FIG. 1. Laboratory coordinates $\{x,y,z\}$, $\mathbf{D}(0)$ input vector, $\mathbf{D}(l)$ output vector, ψ rotation, and $\Delta\psi$ change of rotation of the polarization plane.

$$B = B^{\mathrm{re}} - iB^{\mathrm{re}}GB^{\mathrm{re}}. \tag{2}$$

The matrix G comprises the components G_1, G_2, and G_3 of the gyration vector $\mathbf{G}\|\mathbf{k}$ as

$$G = \begin{pmatrix} 0 & -G_3 & G_2 \\ G_3 & 0 & -G_1 \\ -G_2 & G_1 & 0 \end{pmatrix}. \tag{3}$$

The length of the gyration vector is $|\mathbf{G}| = g_{mn}l_il_j$, where l_i and l_j are the direction cosines of the wave normal $\mathbf{k}$ for $i, j = 1,2,3$. The term B^{re} in the product of the imaginary part of the tensor B in Eq. (2) can be replaced by the unperturbed part B^o since $1/n_o^2 \gg rE_i$. Substituting Eqs. (1) and (3) into Eq. (2) we express the complex impermeability tensor in the principal crystallographic coordinate system $\{x_1,x_2,x_3\}$ as

$$B = \begin{pmatrix} \frac{1}{n_o^2} & rE_3 + i\frac{G_3}{n_o^4} & rE_2 - i\frac{G_2}{n_o^4} \\ rE_3 - i\frac{G_3}{n_o^4} & \frac{1}{n_o^2} & rE_1 + i\frac{G_1}{n_o^4} \\ rE_2 + i\frac{G_2}{n_o^4} & rE_1 - i\frac{G_1}{n_o^4} & \frac{1}{n_o^2} \end{pmatrix}. \tag{4}$$

In order to examine the evolution of polarization, the light beam is analyzed into two eigenstates of polarization $\mathbf{D}_1$ and $\mathbf{D}_2$ that propagate independently. Initially, the impermeability tensor B is transformed to the external laboratory coordinate system $\{x,y,z\}$ (crystal face coordinate system), in which the wave vector $\mathbf{k}$ is parallel to the y axis (Fig. 1). The transformed tensor is

$$B' = ABA^{\mathrm{T}}, \tag{5}$$

where A is the transformation matrix between the crystallographic and the laboratory coordinates. By neglecting the second row and column which correspond to the y direction of propagation, the dimension of B' is reduced, thus resulting in a 2×2 matrix. For $\hat{\mathbf{x}}\|[\bar{1}10]$, $\hat{\mathbf{y}}\|[\bar{1}\bar{1}\bar{1}]$, and $\hat{\mathbf{z}}\|[\bar{1}\bar{1}2]$, and for propagation along y the reduced tensor is

$$B' = \begin{bmatrix} \frac{1}{n_o^2} + \frac{rE_o}{\sqrt{3}} & -i\frac{1}{n_o^4}\left(g_o - \frac{2\zeta E_o}{\sqrt{3}}\right) \\ +i\frac{1}{n_o^4}\left(g_o - \frac{2\zeta E_o}{\sqrt{3}}\right) & \frac{1}{n_o^2} + \frac{rE_o}{\sqrt{3}} \end{bmatrix}. \tag{6}$$

The eigenstates $\mathbf{D}_i$ are calculated from the eigenvalue problem $B'\mathbf{D}_i = 1/n_i^2\mathbf{D}_i$, $i=1,2$. For the particular case of propagation along [111], the solutions of the eigenvalue problem are

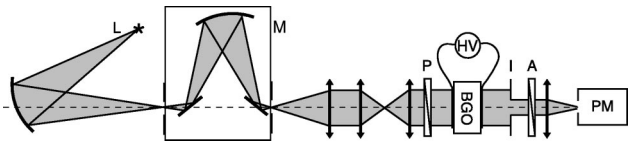

FIG. 2. Schematic diagram of the experimental setup: L incandescent lamp, M grating monochromator, P polarizer, HV high-voltage supply, I iris, A analyzer, and PM photomultiplier.

$$\frac{1}{n_1^2} = \frac{1}{n_o^2} + \frac{rE_o}{\sqrt{3}} - \frac{1}{n_o^4}\left(g_o - \frac{2}{\sqrt{3}}\zeta E_o\right),$$

$$\frac{1}{n_2^2} = \frac{1}{n_o^2} + \frac{rE_o}{\sqrt{3}} + \frac{1}{n_o^4}\left(g_o - \frac{2}{\sqrt{3}}\zeta E_o\right), \tag{7}$$

$$\mathbf{D}_1 = \begin{pmatrix} +i \\ 1 \end{pmatrix},$$

and

$$\mathbf{D}_2 = \begin{pmatrix} -i \\ 1 \end{pmatrix}, \tag{8}$$

where n_1 and n_2 are the refractive indices of the two circularly polarized eigenstates $\mathbf{D}_1$ and $\mathbf{D}_2$ respectively. The composition of the two eigenstates results in the polarization of the transmitted beam which is linear. The rotation of the polarization plane per unit length ϱ is

$$\varrho = \frac{\psi}{l} = \frac{\pi}{\lambda}(n_1 - n_2). \tag{9}$$

Ignoring the EO effect in Eqs. (7) the change of the polarization rotation per unit length that is attributed to the EG effect is thus

$$\Delta\varrho = -\frac{2}{\sqrt{3}}\frac{\pi}{\lambda n_o}\zeta E_o. \tag{10}$$

The derived coefficient $2/\sqrt{3}$ in Eq. (10) is different from the coefficients 1 and $2/(3\sqrt{3})$ reported in Refs. 12 and 13, respectively; the derivation of these coefficients is not included in both papers.

III. EXPERIMENTAL SETUP

Our experimental setup is shown in Fig. 2. An intensity stabilized light beam emitted by an incandescent lamp is filtered using a 2-nm bandpass grating monochromator (M). The collimated beam is linearly polarized by a polarizer (P) and is directed perpendicularly on the BGO crystal. The entrance and exit faces of the crystal are cut and polished parallel to the $(\bar{1}\bar{1}\bar{1})$ plane and the side faces are cut along the $(\bar{1}10)$ and $(\bar{1}\bar{1}2)$ planes. In order to apply electric field along the direction of propagation, a transparent conductive indium tin oxide (ITO) thin film is evaporated on both (111) faces with a surface resistivity of less than 1 $\mathrm{k}\Omega$/square thus forming a capacitor. The thickness of the crystal is $l=4.39$ mm, and the optical window of the conductive film is 8

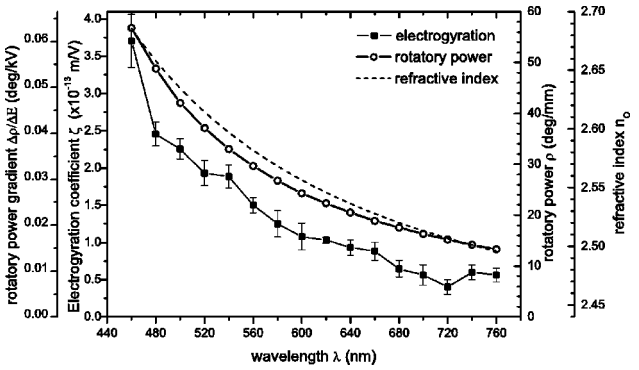

FIG. 3. Electrogyration, optical rotatory power, and refractive index of a BGO crystal in the visible spectral range. Here, ζ left axis inside, $\Delta\varrho/\Delta E$ left axis outside, ϱ right axis inside, and n_o right axis outside. Data for the refractive index n_o are from Ref. 21.

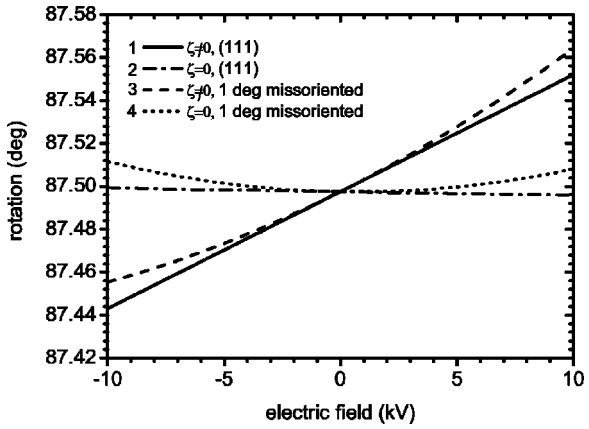

FIG. 4. Rotation of the polarization plane for a 4.39-mm BGO crystal versus the applied electric field at 640 nm: (1) both EG and EO and (2) only EO for (111) cut; (3) both EG and EO and (4) only EO for 1° misoriented (111) cut. Here, $\zeta=0.1$ and $r=3.52$ pm/V.

$\times 9$ mm^2. An iris diaphragm (I) allows only the part of the output beam coming from the central area of the crystal where the electric field is homogenous. The output beam passes through a rotating analyzer (A) mounted on a 0.01°/step motor-driven rotating stage and is collected onto a photomultiplier active surface to measure its intensity. The intensity is a sinusoidal function of the azimuth angle of the analyzer and is recorded at 1° increments. The rotation ψ of the polarization plane is calculated from the phase of the first harmonic of the Fourier series of the sinusoidal intensity. This experimental setup and measurement method allows for higher-precision polarization measurements in comparison with the null intensity phase detection method described in Ref. 13.

IV. RESULTS AND DISCUSSION

In order to calculate the electrogyration coefficient we measure the rotation of the polarization plane per unit length ϱ versus the applied electric field E ranging from -10 to $+10$ kV/cm over the visible spectrum. The relationship between ϱ and E is linear and the electrogyration coefficient ζ is calculated from Eq. (10). In Fig. 3 we present the experimental results for the gradient $\Delta\varrho/\Delta E$ and the electrogyration coefficient ζ at room temperature. It can be observed that the data exhibit spectral dispersion with the value of $\Delta\varrho/\Delta E$ ranging from 0.060°/kV at 460 nm to 0.005°/kV at 760 nm. The value of ζ also ranges from $(3.7\pm0.3)\times10^{-13}$ to $(0.5\pm0.1)\times10^{-13}$ m/V, respectively, for 460–760 nm. The error bars are calculated from the deviation of the measured values from the linear relation between ϱ and E. It can be observed that the error increases with frequency, that is, at the blue-violet end of the spectrum. That is probably caused by the higher absorption in this range which decreases the detected signal-to-noise ratio.

At this point we shall examine some details on the method followed in measuring the EG coefficient. In Refs. 9, 15, and 17 it is reported that the reflections of the propagating beam at the front and the back face of a (110)-cut crystal modify the polarization state of the output beam. However, this cannot be observed in the (111)-cut configuration since the rotation of the polarization plane of the light that bounces back and forth between the input and output face is reversed due to the reciprocity of optical activity and the electrogyratory effect. Consequently, the reflection effects do not alter the polarization of the output beam.

Although in the (111) configuration the electro-optic effect does not affect the circular eigenstates of polarization, the EO coefficient r appears in the eigenvalues [Eqs. (7)], which is finally ignored for the calculation of $\Delta\varrho$ in Eq. (10). In Fig. 4 (curves 1 and 2) we present the rotation ψ of the polarization plane for a BGO crystal versus the applied electric field. It is observed that the electro-optic effect alone (curve 2) modifies the rotation of polarization just slightly. We estimate, however, that its influence is 30 times smaller than the electrogyration effect. Consequently, the omission of the EO term in Eq. (10) is justified.

In the analysis in Sec. II we assume that the crystal is perfectly cut parallel to the (111) plane. At this point we examine the effects of the crystal having a slightly different orientation than (111), which would engage the EO effect into wave propagation. In this case, the configuration of a misoriented crystal is described by a different transformation matrix A [see Eq. (5)], which generally results in elliptic eigenstates of propagation and different refractive indices [Eqs. (7) and (8)]. The rotation of the polarization plane versus the applied electric field for a 1° misoriented crystal is presented in Fig. 4 (curves 3 and 4). It can be observed that the influence of the EO effect alone (curve 4) is parabolic, which means that a possible misorientation would produce a pseudoelectrogyratory effect that would be easily identified by its nonlinearity. Such an effect is negligible compared to the original electrogyration for the known values of r and ζ and for the 1° misoriented crystal.

Finally, the absorption effects were also neglected in describing the impermeability tensor B. Assuming that the absorption is isotropic, an imaginary part κ is added on the diagonal elements of the impermeability tensor B in Eq. (2) which relaxes its Hermitian property. Although the new eigenvalues of the reduced impermeability tensor B' are complex, the eigenstates for the (111) cut remain circularly polarized. The polarization plane rotation is very slightly

influenced, since $n \gg \kappa$ in the spectral range of 460–760 nm (Refs. 22–24) and, most importantly, the gradient $\Delta\varrho/\Delta E$ is not influenced at all.

The experimental value of the electrogyration coefficient at 640 nm that we found ($\zeta = 0.1$ pm/V) is within the boundary $\zeta < 0.35$ pm/V at 633 nm reported by Vachss and Hesselink[17] for BGO. According to the oscillatory model by Miller,[9] the ratio of ζ/r should be analogous to $G/(n^2-1) \simeq 0.8 \times 10^{-4}$; assuming that $r = 3.52$ pm/V, the electrogyration coefficient should be $\zeta = 0.28 \times 10^{-15}$ m/V. This theoretical value is extremely low and is also incompatible with the measured electrogyration coefficients in BSO ($\zeta = 0.952$, 2.0 ± 0.1, and 1.8 ± 0.4 pm/V in Refs. 12, 14, and 16, respectively) and in BTO (0.35 ± 0.01 pm/V in Ref. 15).

The dispersion of the EG coefficient of BGO (Fig. 3) is related to the dispersion observed in optical activity and refractive index near the absorbtion edge which is found to be about 3.2 eV.[22] The electrogyration dispersion has been studied in scheelite and apatite crystals[10,25] only, and has not been detected before in sillenite crystals.[14] According to the microscopic theory of electrogyration by Stasyuk and Kotsur[26] the lattice and ionic contribution to the effect are studied with the help of Green's functions. The theoretical frequency dependence discussed in Ref. 26 is similar to our observed data near the absorption edge.

V. CONCLUSIONS

We have studied and experimentally measured the electrogyration in BGO sillenite crystals. The effect has been observed using the (111) cut where the influence of the electro-optic effect vanishes and thus the direct measurement of the electrogyration coefficient becomes possible. This method provides high accuracy despite the influence of absorption, reflectance, and crystal cut misorientation, and we have achieved the measurement of the electrogyration dispersion near the absorption edge. The electrogyration coefficient was measured and found to range from 0.37 ± 0.03 to 0.05 ± 0.01 pm/V for the 460–760-nm spectrum range. The measured values are within the upper boundaries have been were specified in previous experiments. Finally, the dispersion of the electrogyratory effect appears to follow the dispersion of optical activity and refractive index that is observed in sillenite crystals.

ACKNOWLEDGMENT

One of the authors (N.C.D.) is grateful to the Greek State Scholarship Foundation for financial support.

[1] *Photorefractive Materials and Their Applications, I and II*, Topics in Applied Physics Vol. 61, edited by P. Gunter and J. Huignard (Springer, Berlin, 1988).
[2] P. Yeh, *Introduction to Photorefractive Nonlinear Optics, Wiley Series in Pure and Applied Optics* (Wiley, New York, 1993).
[3] L. Solymar, D. J. Webb, and A. Grunnet-Jepsen, *The Physics and Applications of Photorefractive Materials* (Clarendon, Oxford, 1996).
[4] Y. I. Sirotin and M. P. Shaskolskaya, *Fundamentals of Crystal Physics* (Mir, Moskow, 1982).
[5] I. S. Zheludev, Sov. Phys. Crystallogr. **9**, 418 (1965).
[6] P. V. Lenzo, E. G. Spencer, and A. A. Ballman, Appl. Opt. **5**, 1688 (1966).
[7] P. V. Lenzo, E. G. Spencer, and A. A. Ballman, Phys. Rev. Lett. 19, 641 (1967).
[8] G. F. Moore, P. V. Lenzo, E. G. Spencer, and A. A. Ballman, J. Appl. Phys. **40**, 2361 (1969).
[9] A. Miller, Phys. Rev. B **8**, 5902 (1973).
[10] O. G. Vlokh, Ferroelectrics **75**, 119 (1987).
[11] E. Anastassakis, Appl. Phys. Lett. **21**, 212 (1972).
[12] O. G. Vlokh and A. V. Zarik, Ukr. Fiz. Zh. (Russ. Ed.) **22**, 1032 (1977).
[13] T. J. Tayag, T. E. Batchman, and J. J. Sluss, Appl. Opt. **31**, 625 (1992).
[14] V. V. Kutsaenko and V. T. Potapov, JETP Lett. **43**, 142 (1986).
[15] J. P. Wilde and L. Hesselink, J. Appl. Phys. **67**, 2245 (1990).
[16] K. Nakagawa, N. Kajita, J. Chen, and T. Minemoto, J. Appl. Phys. **69**, 954 (1991).
[17] F. Vachss and L. Hesselink, Opt. Commun. **62**, 159 (1987).
[18] J. F. Nye, *Physical Properties of Crystals* (Oxford University Press, Oxford, 1957).
[19] A. Yariv and P. Yeh, *Optical Waves in Crystals* (Wiley, New York, 1984).
[20] T. A. Maldonado and T. K. Gaylord, Appl. Opt. **28**, 2075 (1989).
[21] D. G. Papazoglou, Ph.D. thesis, Aristotle University of Thessaloniki, 1997.
[22] H. Vogt, K. Buse, H. Hesse, and E. Krätzig, J. Appl. Phys. **90**, 3167 (2001).
[23] J. S. McCullough, A. L. Harmon Bauer, C. A. Hunt, and J. J. Martin, J. Appl. Phys. **90**, 6017 (2001).
[24] V. Marinova, M. Veleva, D. Petrova, I. M. Kourmoulis, D. G. Papazoglou, A. G. Apostolidis, E. D. Vanidhis, and N. C. Deliolanis, J. Appl. Phys. **89**, 2286 (2001).
[25] I. V. Stasyuk and S. S. Kotsur, Phys. Status Solidi B **130**, 103 (1985).
[26] I. V. Stasyuk and S. S. Kotsur, Phys. Status Solidi B **117**, 557 (1983).